Reactive wetting phenomena of MgO−C refractories in contact with CaO−SiO$_2$ slag

Seon-Hwa HEO[1], Kyuyong LEE[2], Yongsug CHUNG[1]

1. Department of Advanced Materials Engineering, Korea Polytechnic University,
Siheung-City, Gyeonggi-Do 429-793, Korea;
2. Department of Consilience, Korea Polytechnic University,
Siheung-City, Gyeonggi-Do 429-793, Korea;

Abstract: Wetting phenomena between MgO−C and CaO−SiO$_2$ slags were investigated by varying carbon content. A sessile drop technique was adopted to study the wetting phenomena in conjunction with a high speed camera for the observation of intrinsic wetting phenomena. The results show that the high content of SiO$_2$ and the presence of Al$_2$O$_3$ in slags enhance the diffusion of Mg^{2+}, leading to the promotion of reactive wetting. The carbon in MgO−C refractory impedes the penetration of slags by repelling the slag and slowing the diffusion of Mg^{2+}. This accounts for the non-wetting behavior of the slag on MgO−C refractory with 17% (mass fraction) carbon similar to that of graphite.

Key words: MgO−C refractory; molten slags; wetting; penetration

1 Introduction

Magnesia (MgO) and mag−carbon (MgO−C) are widely used as metal-making refractory. MgO refractory can be wetted, dissolved and corroded when it is in contact with oxide slags. On the other hand, the behavior of MgO−C refractory is different because of carbon. The carbon plays an important role in penetration of the slags into refractories due to its non-wetting property. In metal-making process, various corrosion mechanisms of the MgO−C refractory due to the slag exist, such as erosion, penetration and dissolution. The wettability of the liquid slag on refractory considerably affects the slag penetration [1−9].

In penetration of the slag into the refractory, the absorption force of capillary phenomena is determined by the surface tension and the contact angle of the slag on the refractory. Figure 1 shows a schematic diagrams of the relation between the contact angle and the penetration of the liquid into the pore following

$$\Delta P = (2\gamma_{LV} \cdot \cos\theta)/r \tag{1}$$

where ΔP is absorption force of capillary phenomena, γ_{LV} is the surface tension of liquid−vapor, θ is the contact angle, and r is the radius of capillary [10].

Another wetting property is spreading characteristic of slag. It suggests that the work of adhesion is the work per unit area necessary to reversibly separate a liquid from a solid [11]. Young-Dupre equation,

$$W_{SL} = \gamma_{LV}(1 + \cos\theta) \tag{2}$$

The work of adhesion (W_{SL}) is determined as a function of contact angle and surface tension of the liquid−vapor interface. Considering the separation of a liquid, the reversible work required to create unit area of liquid surface is

$$W_{LL} = 2\gamma_{LV} \tag{3}$$

The energy difference is defined as the spreading coefficient, $S_{L/S}$:

$$S_{L/S} = W_{SL} - W_{LL} \tag{4}$$

Figure 2 shows the process for the work of spreading. If $S_{L/S}$ is zero, i.e., $W_{SL} = W_{LL}$, the interaction between solid and liquid is equal to the interaction between liquid and liquid, and complete wetting occurs. On the other hand, if $S_{L/S}$ is strongly negative,
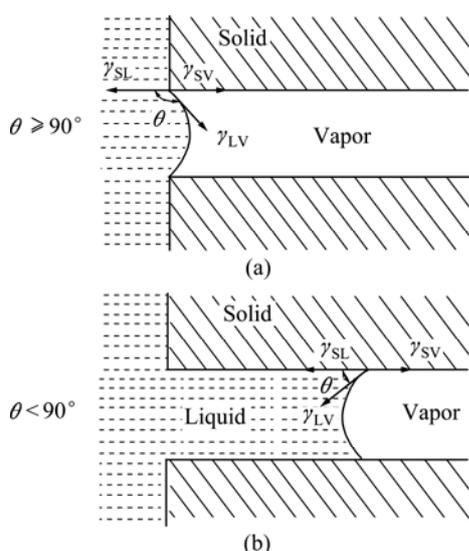
Fig. 1 Schematic diagrams of relation between contact angle and penetration in solid−liquid−vapor phase
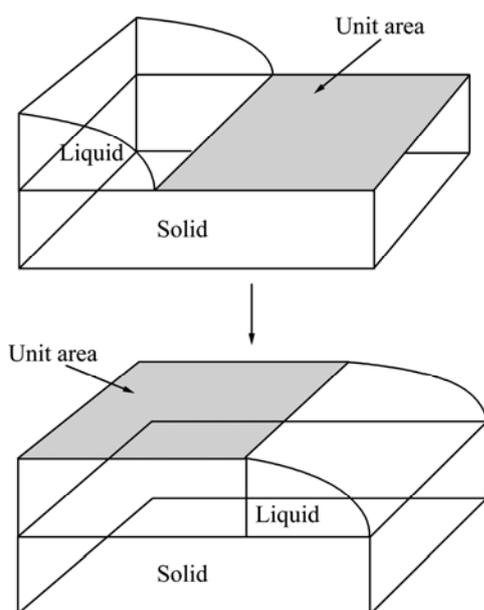

Fig. 2 Schematic diagrams of process for spreading

i.e., $W_{LL} \gg W_{SL}$, the interaction between liquid and liquid is much stronger than the one between solid and liquid, and generates the non-wetting condition [11].

Several studies on wetting of MgO or graphite refractories by molten slags have been published [12−14]. SHEN et al [12] investigated the system of 38.7%SiO$_2$−44.3%MnO−11.4%TiO$_2$−5.6%FeO$_x$ (mass fraction) slag on an MgO substrate and obtained 8° for the contact angle at 1200 °C for 10 min. On the other hand, in the case of the graphite substrate, the contact angle varies in the range 109°−135° depending on the temperature and chemical composition, showing a tendency of non-wetting. For the system of 38.7%SiO$_2$−44.3%MnO−11.4%TiO$_2$−5.6%FeO$_x$ slag on a graphite substrate,

SHEN et al [12] obtained 109° for the contact angle at 1400 °C for 30 min. SUN et al [13] investigated the systems of 37.3%MnO−33.4%SiO$_2$−18.4%CaO−9.6% Al$_2$O$_3$ slag and 13.9%MnO−46.1%SiO$_2$−25.3%CaO−13.4%Al$_2$O$_3$ slag on graphite substrates, and the contact angles were 126.5° and 134°, respectively, at 1550 °C for 1−3 h. The system of SiO$_2$−13.4%Na$_2$O−10.9%CaO−1.4%MgO−1.6%Al$_2$O$_3$ slag on a graphite substrate was investigated by PECH et al [14] that the contact angle is 135° at 1034 °C for 20 min. Since the experimental condition, such as slag composition, temperature and reaction time between the substrate and slag causes the large deviation in the contact angle, it is difficult to determine an intrinsic value of wetting angle. In this study, reactive wetting phenomena between MgO−C and CaO−SiO$_2$ slags were investigated using a sessile drop technique. The carbon content in MgO−C refractories was varied to observe the effect of carbon on wetting phenomena. Using a high speed camera (up to 1000 frame per second), the initial wetting was observed to obtain the intrinsic value of wetting angle, and also the long term wetting behavior was observed to investigate reactive wetting phenomena.

2 Experimental

2.1 Materials

Four types of refractories, such as pure graphite, MgO−17%C, MgO−4%C and pure MgO, were used. The chemical composition of each refractory is shown in Table 1. Two types of slags were used, and the chemical composition of each slag is shown in Table 2. All the refractory substrates were cut to have rectangular dimensions of approximately 20 mm×20 mm×10 mm and polished on one side to be contacted by the slag.

2.2 Experimental procedures

The experimental apparatus for the sessile drop technique (SDT) is shown in Fig. 3. High speed camera

Table 1 Chemical composition of MgO−C refractories (mass fraction, %)

Material	Mass fraction/%		Impurity (mass fraction)	Remark
	MgO	C		
Graphite	−	99.9	0.1%	Alfa Aesar., USA
MgO−17%C	82.18	17.00	0.54%CaO−0.26%SiO$_2$−0.02%Fe$_2$O$_3$	
MgO−4%C	95.18	4.00	0.54%CaO−0.26%SiO$_2$−0.02%Fe$_2$O$_3$	
MgO	99.9	−	0.1%	Toda., Japan

Table 2 Chemical composition of slags (mass fraction, %)

Slag	Basicity	Composition/%		
		CaO	SiO$_2$	Al$_2$O$_3$
CaO−SiO$_2$	0.8	45.0	55.0	−
CaO−SiO$_2$−Al$_2$O$_3$	0.8	40.0	50.0	10.0
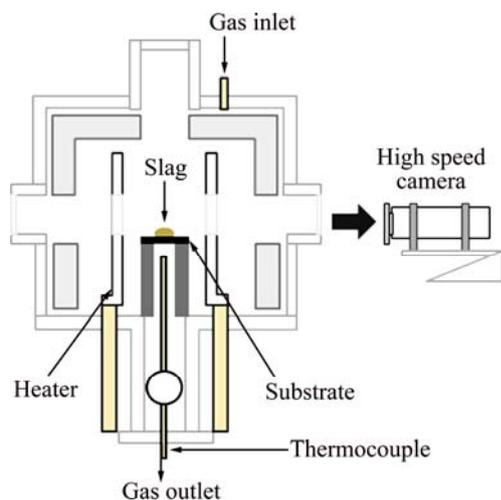
Fig. 3 Schematic diagram of experimental setup of SDT

was used to capture both the initial contact angle at the rate of 1000 frames per second and the long-term change of the contact angle due to reactive wetting. Dedicated software was used to extract the contact angle and surface tension.

The furnace temperature was elevated to 1600 °C at the rate of 10 °C/min. The reaction chamber was sealed and evacuated to 1.33 Pa with a rotary vacuum pump. Then, it was flushed two times and filled with purified 10%H$_2$−Ar gas to $1.01×10^5$ Pa. At 1600 °C, a drop of completely melted liquid slag was dropped onto the substrate, which is very different from the conventional SDT. In the conventional SDT method, solid-state slag is placed on the substrate at the room temperature, and then is melted with the temperature of the chamber increasing, therefore, it is inevitable to have the chemical composition change that already occurs by the solid−solid diffusion during the period of heating. Figure 4

shows sequential images of the slag droplet captured by the high speed camera in both the conventional and the new SDT methods. In the new SDT method, any earlier change of chemical composition is prohibited, and the very initial dynamics of the wetting can be observed from the moment of the contact of the slag with the substrate.

3 Results and discussion

3.1 Effect of chemical composition of slag on wettability with MgO−17%C

Change of the contact angle with time on the MgO−17%C substrate is observed for the two types of slags with different chemical compositions. Figure 5 shows the change of contact angles in 60 min. The contact angle drastically decreases by chemical dissolution at the initial time. However, the contact angle gradually decreases by reactive diffusion at latter part.

Because of the ionic nature of molten slags, the diffusive mass transfers by ions. The ionic diffusivities are measured using radioactive trace elements dissolved in an oxidized form in the melt. Typical ionic diffusivities of Mg^{2+} in slags ($D_{MgO-(CaO/SiO_2)}$) at 1600 °C are $6×10^{-6}$−$1×10^{-5}$ cm^2/s. Since the electro neutrality must be maintained, diffusion of a cation is accompanied by diffusion of the oxygen ion. The diffusion that occurs in the dissolution of a solid oxide in the slag is controlled by the mobility of the O^{2-} ion, which is smaller than the divalent cations [14]. This explains why the contact angle is lowered in the presence of Al$_2$O$_3$ in the CaO−SiO$_2$−Al$_2$O$_3$ slag as show in Fig. 5.

The contact angles for both slags during initial 4 s are shown in Fig. 6. The initial contact angles are quite stable in time scale of seconds, implying that they are the intrinsic values: 92° for the CaO−SiO$_2$ slag and 50° for the CaO−SiO$_2$−Al$_2$O$_3$ slag. The transient decrease of the contact angle for CaO−SiO$_2$ slag during initial 2 s is caused by the mechanical stabilization due to gravity, not by the reactive diffusion.
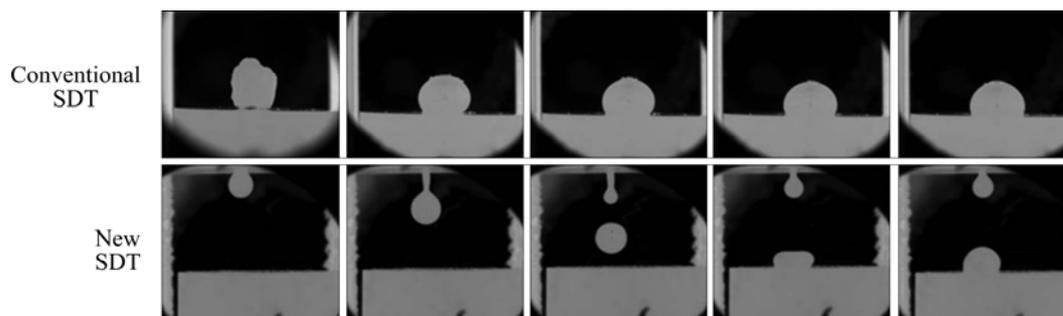
Fig. 4 Sequential images of slag droplet in conventional and new SDT methods
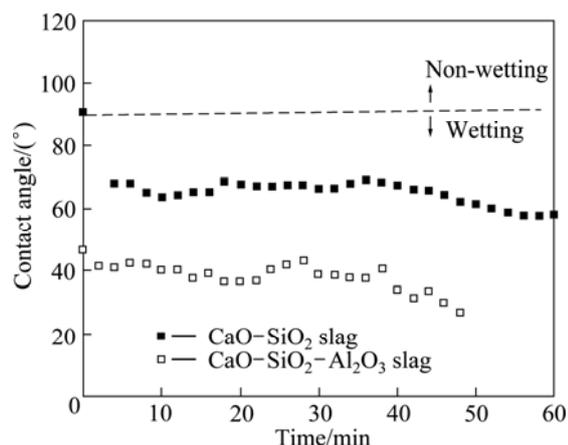
Fig. 5 Long-term change of contact angle for two types of slags on MgO−17%C substrate
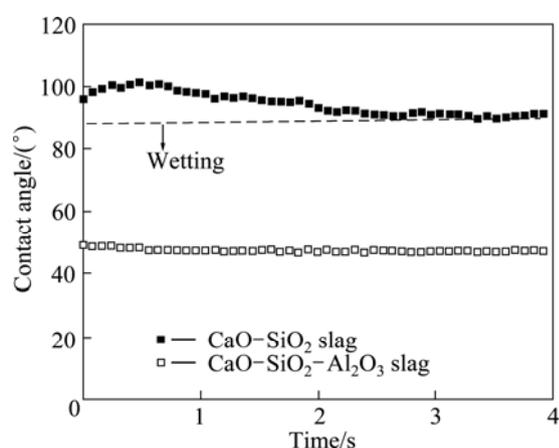

Fig. 6 Initial contact angle for two types of slags on MgO−17%C substrate

3.2 Effect of carbon content in refractory on wettability of CaO−SiO₂ slag

Change of the contact angle with time on various refractory substrates is observed for the CaO−SiO₂ slag. Figure 7 shows the change of contact angles during 60 min. The contact angles during initial 4 s are shown in Fig. 8. The CaO−SiO₂ slag on the pure graphite and MgO−17%C substrates has non-wetting property during initial 4 s. The initial contact angles are 115° for the pure graphite, 92° for MgO−17%C, 40° for MgO−4%C and 10° for the pure MgO substrates, showing that the

contact angle increases with increasing the carbon content in MgO−C. Also, the increase of carbon content in MgO−C reduces the reaction speed so that the contact angle reaches the stable state more slowly, as shown in Fig. 7. These imply that carbon impedes the penetration of slags by repelling the slag and slowing the diffusion of Mg^{2+}.

Figure 9 shows the images of the CaO−SiO₂ slag on various refractory substrates at 1 s after the initial contact. It clearly shows that the contact angle decreases with decreasing carbon content in the refractory substrate. In Fig. 10, contact angle data in this study and the references are plotted together. The data in this study are
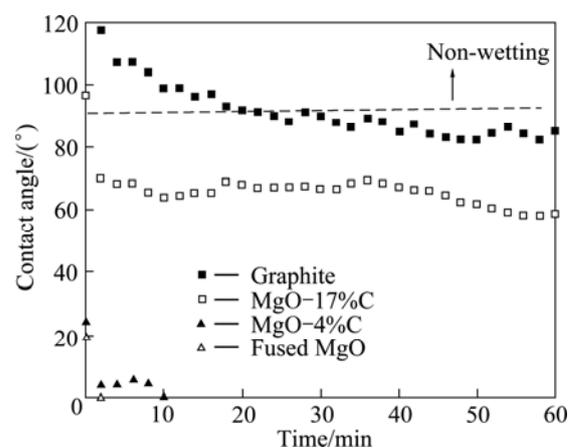

Fig. 7 Long-term change of contact angle for CaO−SiO₂ slag on various substrates
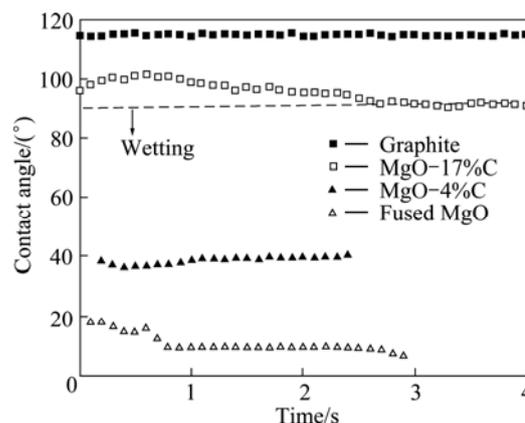

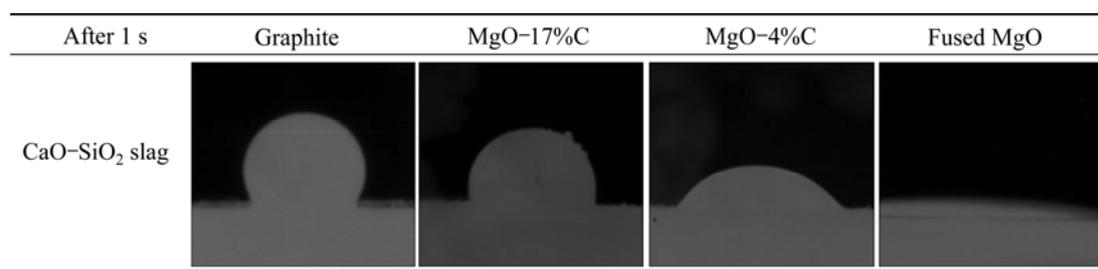**Fig. 8** Initial contact angle for CaO−SiO₂ slag on various substrates

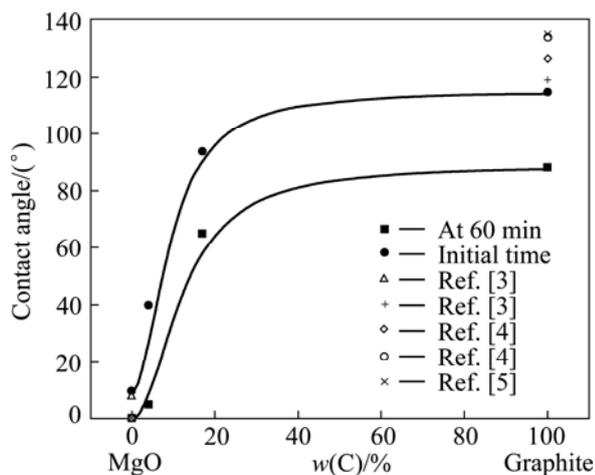**Fig. 9** Images of CaO−SiO₂ slag on various substrates after initial 1 s

Fig. 10 Contact angle data in this study and references

lower than the data in the references. The reason is that the temperature in this study (1600 °C) is higher than in the references (1034−1550 °C) [12−14]. In addition, the higher content of SiO_2 and the presence of Al_2O_3 in the slags used in this study also contribute to the decrease of contact angles.

3.3 Phase diagram analysis of CaO−SiO₂−MgO
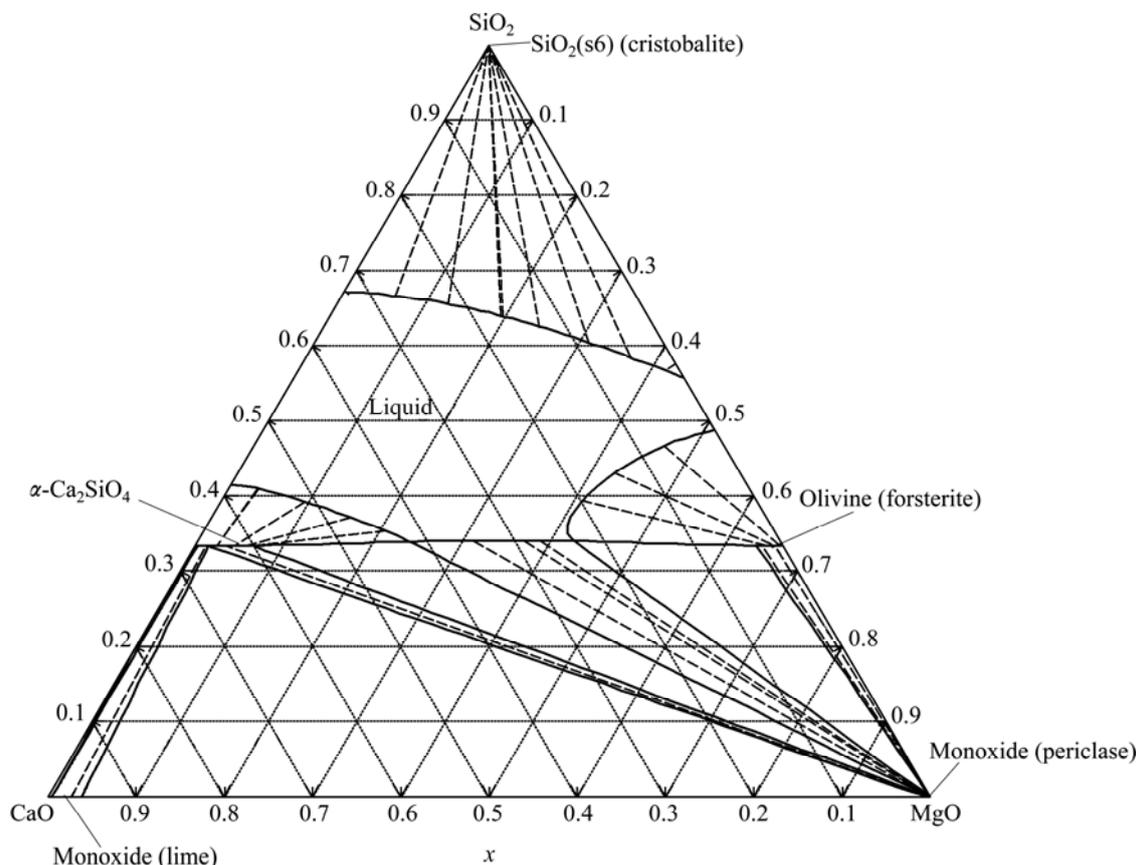
Figure 11 shows the ternary phase diagram of

CaO−SiO₂−MgO at 1600 °C obtained by Factsage. For the chemical composition of the CaO−SiO₂ slag, MgO saturation content is 0.26 mole (9.4%, mass fraction) from the phase diagram. The diffusion of MgO occurs until its saturation. As Mg^{2+} ions diffuse into the slag, the wettability increases.

3.4 Analysis on penetration of CaO−SiO₂ slag into various refractories

Figure 12 shows a plot of the absorption force as a function of time for CaO−SiO₂ slag on various substrates obtained by Eq. (1). As mentioned above, the absorption force, which is the driving force for penetration, is affected by the surface tension and the contact angle. The plot shows that the absorption force increases with time, leading to higher penetration.

Figure 13 shows the spreading coefficient for CaO−SiO₂ slag on various refractories obtained by Eqs. (2), (3) and (4). The spreading coefficient closing zero promotes the wetting of the substrate by the liquid. The plot shows that the spreading coefficients in all cases are approaching to zero with time. However, the higher the carbon content in the substrate is, the more slow the spreading coefficient approaching to zero is, which indicates that carbon delays the spreading of the slag, and therefore suppresses the penetration.
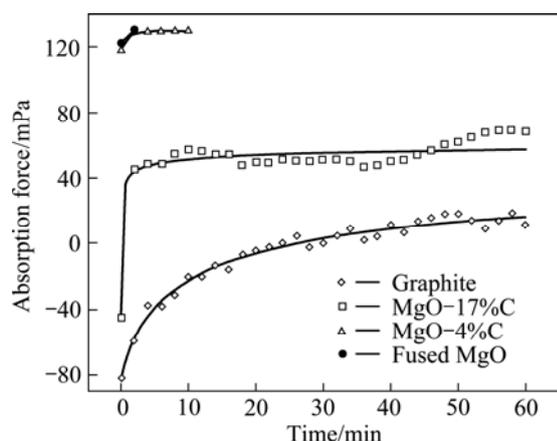

Fig. 11 Ternary phase diagram of CaO−SiO₂−MgO at 1600 °C (FACTSAGE)

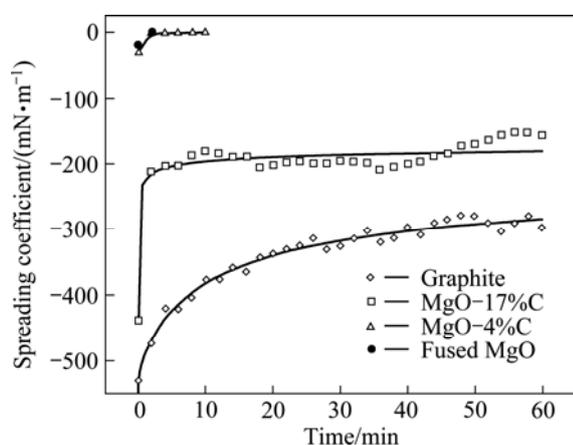**Fig. 12** Absorption force for CaO−SiO$_2$ slag on various substrates

Fig. 13 Spreading coefficient for CaO−SiO$_2$ slag on various substrates

4 Conclusions

1) The contact angle drastically decreases due to chemical dissolution at the initial time, and then gradually decreases due to reactive diffusion.

2) The high content of SiO$_2$ and the presence of Al$_2$O$_3$ in slags enhance the diffusion of Mg^{2+}, leading to the promotion of reactive wetting.

3) The carbon in MgO−C refractory impedes the penetration of slags by repelling the slag and slowing the diffusion of Mg^{2+}.

4) As the carbon content in MgO−C refractory increases, the absorption force and the spreading of the slag decrease, and therefore the penetration is suppressed.

When the carbon content in MgO−C refractory is about 17% (mass fraction), the slag shows non-wetting behavior on the refractory as on the graphite.

References

[1] MUKAI K. Wetting and marangoni effect in iron and steelmaking processes [J]. ISIJ International, 1991, 32(1): 19−25.

[2] LIU J, GUO M, JONES P T, VERHAEGHE F, BLANPAIN B, WOLLANTS P. In situ observation of the direct and indirect dissolution of MgO particles in CaO−Al$_2$O$_3$−SiO$_2$-based slags [J]. Journal of the European Ceramic Society, 2007, 27: 1961−1972.

[3] KISTLER S F. Wettability [M]. New York: Taylor & Francis Group, 1993: 311.

[4] BLAKE T D. Wettability [M]. New York: Taylor & Francis Group, 1993: 251.

[5] de GENNES P G. Wetting: Statics and dynamics [J]. Reviews of Modern Physics, 1985, 57: 827.

[6] HOCKING L M, RIVERS A D. The spreading of a drop by capillary action [J]. Fluid Nech, 1982, 121: 425.

[7] HOFFMAN R. A study of the advancing interface [J]. Colloid Interface Sci, 1975, 50: 228.

[8] MARMER A. Equilibrium and spreading of liquids on solid surfaces [J]. Advances in Colloid and Interface Science, 1983, 19: 75.

[9] CHUNG Y, CRAMB A W. Dynamic and equilibrium interfacial phenomena in liquid stell-slag systems [J]. Metallurgical and Materials Transactions B, 2000, 31: 957−971.

[10] TSYPKIN G G, CALORE C. Role of capillary forces in vapour extraction from low-permeability, water-saturated geothermal reservoirs [J]. Geothermics, 2003, 32: 219−237.

[11] CHUNG Y, CRAMB A W. Surface and interfacial properties of Fe−30%Cr−S alloys in contact with alumina [J]. Steel Research, 1999, 70: 8−9.

[12] SHEN P, FUJII H, NOGI K. Wettability of some refractory materials by molten SiO$_2$−MnO−TiO$_2$−FeO$_x$ slag [J]. Materials Chemistry and Physics, 2009, 114: 681−686.

[13] SUN H, LONE M, GANGULY S, OSTROVSKI O. Reaction of manganese containing slag with carbon substrate [C]// The Twelfth International Ferroalloys Congress. Helsinki, 2010: 557−567.

[14] PECH J, BRACCINI M, MORTENSEN A, EUSTATHOPOULOS N. Wetting, interfacial interactions and sticking in glass/steel systems [J]. Materials Science and Engineering A, 2004, 384: 117−128.

[15] TURKDOGAN E T. Fundamentals of steelmaking [M]. London: Inst of Materials Ashgate, 1996: 176−177.

(Edited by LI Yan-hong)